

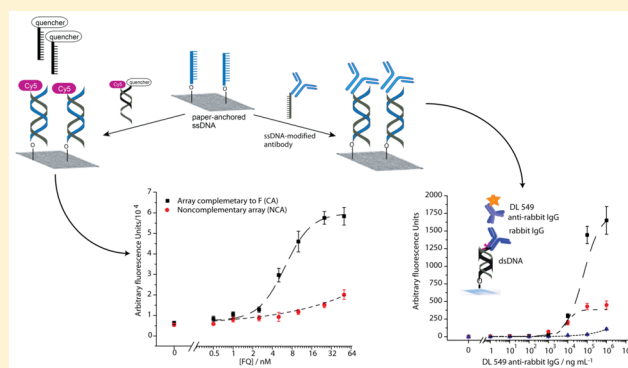
## Analytical Devices Based on Direct Synthesis of DNA on Paper

Ana C. Glavan,<sup>†</sup> Jia Niu,<sup>†</sup> Zhen Chen, Firat Güder, Chao-Min Cheng, David Liu,<sup>\*</sup> and George M. Whitesides<sup>\*</sup>

Department of Chemistry &amp; Chemical Biology, Harvard University, Cambridge, Massachusetts 02138, United States

## S Supporting Information

**ABSTRACT:** This paper addresses a growing need in clinical diagnostics for parallel, multiplex analysis of biomarkers from small biological samples. It describes a new procedure for assembling arrays of ssDNA and proteins on paper. This method starts with the synthesis of DNA oligonucleotides covalently linked to paper and proceeds to assemble microzones of DNA-conjugated paper into arrays capable of simultaneously capturing DNA, DNA-conjugated protein antigens, and DNA-conjugated antibodies. The synthesis of ssDNA oligonucleotides on paper is convenient and effective with 32% of the oligonucleotides cleaved and eluted from the paper substrate being full-length by HPLC for a 32-mer. These ssDNA arrays can be used to detect fluorophore-linked DNA oligonucleotides in solution, and as the basis for DNA-directed assembly of arrays of DNA-conjugated capture antibodies on paper, detect protein antigens by sandwich ELISAs. Paper-anchored ssDNA arrays with different sequences can be used to assemble paper-based devices capable of detecting DNA and antibodies in the same device and enable simple microfluidic paper-based devices.



Microarrays are convenient tools for the multiplex analysis of several biological samples in clinical diagnostics.<sup>1,2</sup> A microarray is a solid support bearing microscopic features that can detect specific target molecules and generate diagnostic data.<sup>3</sup> The standard method of fabrication for microarrays is pin-spotting—a method in which a robotic system deposits small volumes of a solution containing a probe (usually DNA, RNA, antibody, or protein) onto a glass, silicon, or polymer-based substrate.<sup>4</sup> Alternative methods include microstamping, inkjet printing, laser writing, or electrospray deposition, among others.<sup>5,6</sup> These substrates can be derivatized with poly-L-lysine, polyamidoamine dendrimer, amino-terminated silanes, aldehydes, carboxylic acids, or other reactive groups that facilitate attachment.<sup>7</sup> Existing methods for the fabrication of microarrays rely on complex equipment for processing and require a series of lengthy purification and functionalization steps; the substrates commonly used are neither flexible nor inexpensive and are difficult to integrate in low-cost diagnostics systems intended for use in resource-limited settings.

Paper-based microfluidic systems ( $\mu$ PADs)<sup>8–17</sup> have emerged in recent years as a promising technology to address the growing need for simple, quantitative, point-of-care diagnostic devices capable of detecting different analytes from the same specimen in a single run.<sup>17</sup> Paper is a useful substrate for the fabrication of microarrays through its high surface area (due to its high surface roughness and internal porosity) and high density of accessible hydroxyl functional groups.<sup>18</sup> Paper is also inexpensive, flexible, easily shaped by cutting or folding, and disposable by incineration.<sup>17</sup>

To carry out separate assays simultaneously with minimal cross talk on a micro paper-based analytical device (a  $\mu$ PAD), distinct microzones must vary either in terms of access to stored reagents required for the detection of each target or in their affinity for the target molecule. The first approach has received significant attention following the development of 3D  $\mu$ PADs—systems that distribute the sample via vertical flow to independent test zones that store distinct reagents.<sup>11,13</sup> The second approach has, so far, been largely ignored, probably due to the scarcity of methods available for assembling high quality microarrays on paper. To enable sensitive assays, these microarrays must be immobilized (preferably covalently, or, if noncovalent, with very low dissociation constants) and at high density on the surface of the substrate.<sup>18,19</sup>

This manuscript demonstrates the efficient synthesis of DNA oligomers 32 nucleotides in length on the surface of paper and the assembly of the DNA-conjugated papers into paper-based devices that integrate nucleic acid and protein arrays. First, we demonstrate that the arrays of ssDNA can be used to detect fluorescently labeled DNA oligomers in solution. Next, we show that we can produce arrays of proteins and antibodies that are 2 orders of magnitude more dense (based on projected footprint) than microarrays fabricated by pin-spotting.<sup>4</sup> We transformed the paper-anchored ssDNA arrays into antibody arrays via complementary-strand hybridization with

Received: July 26, 2015

Accepted: November 26, 2015

Published: November 26, 2015

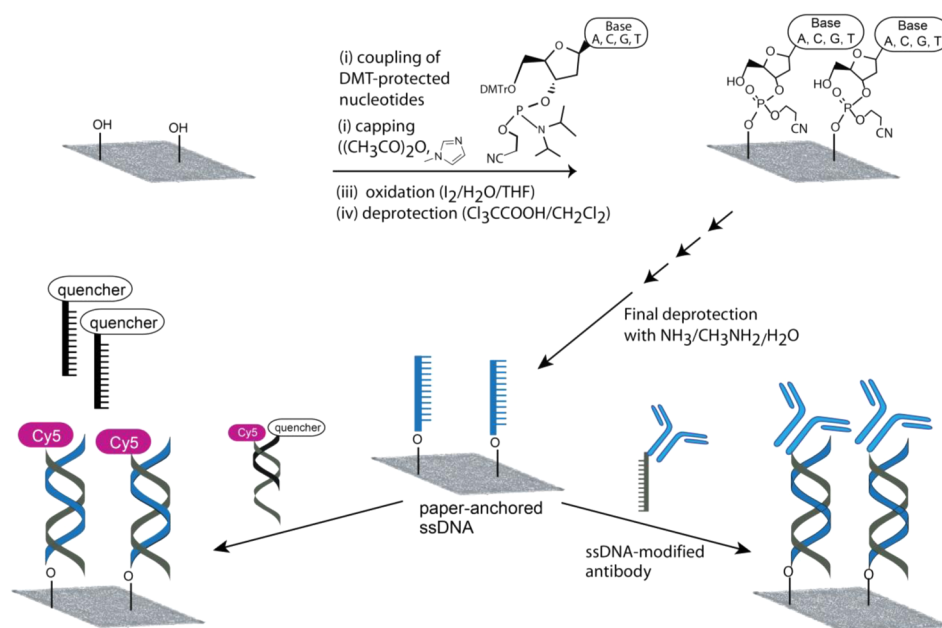


**Figure 1.** Schematic representation of DNA synthesis on paper and its applications to nucleic acid detection and formation of antibody and protein arrays.

ssDNA-conjugated antibodies and show that these arrays of capture antibodies can be used to increase the sensitivity of paper devices. Last, we show that we can use paper-anchored ssDNA arrays with different sequences to assemble paper-based devices capable of detecting DNA and antibodies in the same device.

The technique we used to fabricate DNA arrays takes advantage of the ease with which the surface of paper can be modified to synthesize oligomers of single-stranded DNA (ssDNA) directly. The synthesis of DNA on unmodified paper eliminates potentially time-consuming and costly purification procedures and simplifies downstream processing. To expand the potential impact of these arrays in low-cost, point-of-care clinical diagnostics, we transformed the DNA arrays into protein arrays in situ using a technique developed by Jiang and Heath<sup>20–23</sup> for use on the surface of silicon, glass, PDMS, and other synthetic polymers.<sup>24–31</sup> The technique uses an antibody that is chemically linked to ssDNA and is complementary to a surface-bound ssDNA; the antibody is immobilized on the surface via sequence-specific hybridization. DNA-directed immobilization reduces protein denaturation and enables greater orientational freedom of the antigen-binding sites than either covalent immobilization or nonspecific adsorption and yields a larger proportion of immobilized proteins (antibodies or antigens) that have unhindered binding domains.<sup>25,32</sup> Other advantages of DNA-directed immobilization include increased homogeneity and reproducibility and the consumption of less antibody per experiment.<sup>32</sup>

## RESULTS AND DISCUSSION

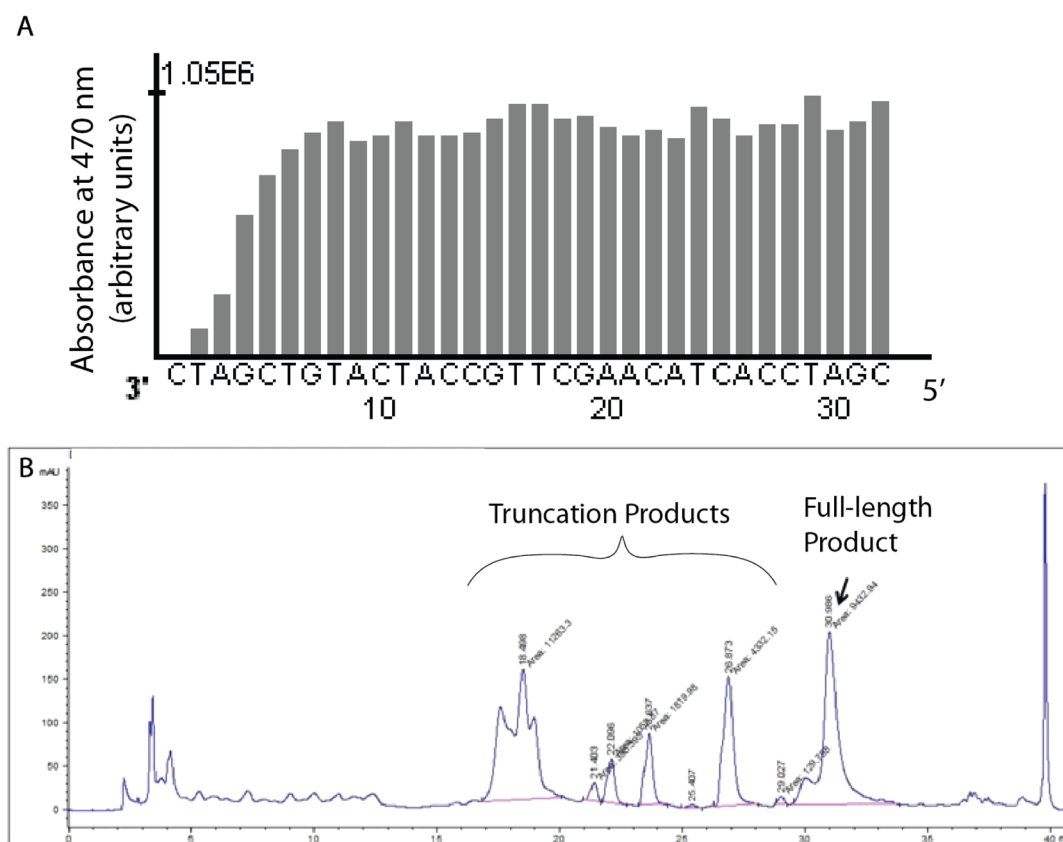
**Direct Synthesis of Single-Stranded Oligonucleotides using Paper as the Solid Support.** The high density of hydroxyl groups on the surface of cellulose paper makes it a useful substrate for the chemistry of phosphoramidite synthesis of ssDNA.<sup>33,34</sup> Whatman chromatography paper has a relatively uniform structure (compared to other papers in terms of pore size, roughness, and anisotropy<sup>12,35</sup>) and is free of coatings or binders that could interfere with the synthesis process.

Figure 1 outlines the procedure used for the solid-phase synthesis of DNA carried out using paper as solid support. The postsynthesis deprotection is carried out in situ, and the process does not require purification steps.

Current methods for fabrication of DNA microarrays require synthesis of DNA on-bead, deprotection, and cleavage from the bead, purification by HPLC, and spotting on substrate. The low cost of the paper support ( $\$0.0007/\text{cm}^2$  Whatman Chr 1 chromatography paper) and the lack of pre- or postsynthesis steps required to activate the substrate or purify the products make the process simple and cost-effective; we believe that this method is compatible with processing on a large scale.

The high surface roughness of the paper, and its porosity, increase the area accessible to reagents and allow for larger numbers of oligonucleotides to be synthesized per area (calculated based on its planar projected footprint) than on a flat substrate (e.g., glass or polymer) with the same surface chemistry. On other substrates, increasing surface area (by applying acrylamide gels to glass slides, for example) to allow the immobilization of larger amounts of DNA resulted in greater signal intensities and an increased dynamic range.<sup>36</sup> We took advantage of the high surface area of the paper by using a paper with a relatively high profile root-mean-square roughness parameter,  $R_{\text{RMS}}$  of  $6.4 \pm 1.9 \mu\text{m}$ , area root-mean-square roughness parameter  $S_{\text{RMS}}$  of  $10.7 \pm 0.6 \mu\text{m}^2$ , and porosity, or volume fraction of void, of  $\sim 68\%$ .<sup>37</sup> Although the real surface area is usually proportional to the surface roughness, the real surface area of a rough surface is challenging to quantify;<sup>38</sup> because the measurements used in fluorescence and colorimetric assays refer to intensity per two-dimensional area, we quantified the surface density of nucleotides in terms of nucleotides per projected (also referred to as plane, flat, or apparent) area of paper.

The terminal DMT protective group of the oligonucleotide, if not cleaved at the end of the synthesis, provided a useful way of characterizing the density of the oligonucleotide on the apparent surface of paper (Figure 2). The cleavage of the terminal DMT under acidic conditions can be monitored at 495 nm by a UV



**Figure 2.** Synthesis of DNA oligonucleotides on paper. (A) The absorbance at 470 nm, produced by the release of DMT carbocation after the coupling of a nucleotide, is used to monitor the yield of each nucleotide addition step. The sequence used in this study was 5'-CGATCCACTACAAGCTTGCATCATGTGCGATC-3'. (B) HPLC trace of DNA fragments cleaved from the paper by reducing the disulfide bridge (the sequence is 5'-CGATCCACTACAAGCTTTTSTTTTTTTTTTTTTTTT-3'). The arrow indicates the peak of the full-length oligonucleotide product. Other marked peaks indicate truncation oligonucleotide products.

spectrometer.<sup>39</sup> The surface density,  $\rho_{\text{SP}}$  (defined as the number of molecules of oligomer per  $\text{cm}^2$  of projected area  $S_p$ ) can be obtained from the UV absorbance at 495 nm,  $A_{495}$ , using eq 1, where  $\epsilon$  is the molar absorptivity of DMT,  $v$  is the volume of the solution in which the DMT is cleaved,  $d$  is the optical path length, and  $N_A$  is Avogadro's number.

$$\rho_{\text{SP}} = \frac{A_{495\text{nm}} \times v \times N_A}{\epsilon \times S_p \times d} \quad (1)$$

Using eq 1 for  $\epsilon$  of DMT  $7.2 \times 10^4 \text{ L mol}^{-1} \text{ cm}^{-1}$ ,<sup>39</sup> we estimated the density of oligonucleotides per projected area of paper to be  $4.5 \pm 0.5 \times 10^{14} \text{ cm}^{-2}$ . This value is 2 orders of magnitude higher than that of the current standards for DNA immobilization on 2-D substrates (for example, using pin spotting or adsorption on poly-L-lysine coated glass slides).<sup>4</sup> With the exception of the first five coupling cycles, the UV absorbance at 495 nm of the DMT cleavage solution has plateaued, indicating that the phosphoramidite coupling and deprotection reactions occurred efficiently during the synthesis. The lower coupling efficiency observed in the first five coupling steps can be attributed to sluggish reactions of the DNA phosphoramidites to the less-accessible hydroxyl groups buried in the paper fibers. Because extending the reaction time of the initial coupling rounds did not improve the coupling yields, we introduced spacer nucleotides of ten nucleotides at the 3' end of the directly synthesized oligonucleotide on paper and designed the probe-binding region to be located at the 5' end.

To confirm the identity of the full-length DNA oligonucleotide generated by synthesis on paper and measure the yield, we introduced a cleavable disulfide bond in the sequence. After completing the synthesis, the terminal DMT group was left on for use as an HPLC handle. The paper-anchored DNA oligonucleotide was cleaved by reduction of the disulfide group with dithiothreitol (DTT), and the eluted material was subjected to HPLC. The main HPLC peaks were analyzed by electrospray ionization mass spectrometry (ESI-MS). Mass spectroscopy confirmed that the HPLC peak eluting at 30.9 min (Figure 2) with a mass of 6217.9 Da was within 1.0 Da of the expected mass (with  $^{13}\text{C}$  isotope correction), 6217.1 Da, of the full-length product after cleavage. The yield of the desired full-length oligonucleotide was estimated using absorbance data at 260 nm, as the ratio of the area of the peak corresponding to the full-length oligonucleotide (confirmed by mass spectrometry) and the sum of the areas of the peaks in the chromatogram corresponding to truncation and full-length products. The ratio of the amount of full-length product to the total amount of oligonucleotides cleaved and eluted from the paper substrate is 32% according to HPLC.

**Use of ssDNA Arrays to Detect Fluorescently Labeled Oligonucleotides.** To minimize the effects of nonspecific adsorption, we used a competitive assay to detect a fluorescently labeled target oligonucleotide, F. A Cy5 reporter was attached to the 5' end of the target. F is also complementary to the DNA oligomer S1 synthesized directly on the surface of the paper. A paper-anchored array of an oligomer S2 (see Table S-1

for full sequence), with a sequence noncomplementary to F, was used as a negative control.

A short ssDNA probe, Q, was designed to be complementary to F and labeled with a dark quencher (Iowa Black RQ) at the 3' end. F and Q were mixed in a 1:9 ratio and allowed to hybridize by heating to 37 °C, and the solution was then allowed to cool to room temperature. When F and Q hybridize, the fluorophore (Cy5) on F is brought in close proximity to the quencher (Iowa Black RQ), and the hybridized product does not fluoresce.

The ssDNA anchored on the paper surface was designed to have a higher affinity for F than for the probe Q. The assay is based on the competition between the DNA oligomer anchored on the paper microzone and Q for hybridization with F; blocking and washing steps are not required because a fluorescent signal is produced only as the ssDNA synthesized on paper displaces Q (from the FQ complex) to hybridize with F.

Figure 3 shows the fluorescent signal recorded after solutions of the FQ complex in concentrations between 50 nM and 500 pM

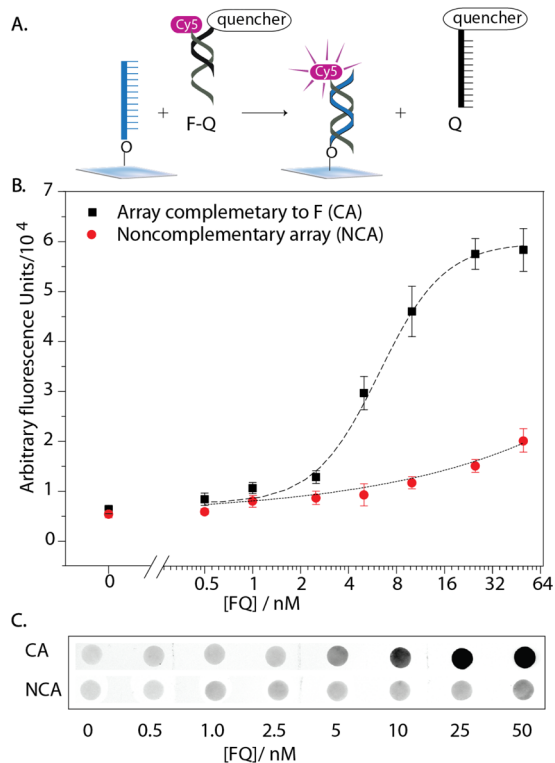


**Figure 3.** Fluorescence-based detection of DNA oligonucleotides using strand displacement within paper-anchored ssDNA arrays. The sequence S1 used for the DNA array (CA) is complementary to the target DNA oligomer F, whereas the sequence S2 used for a control array (NCA) is orthogonal to F. Solution FQ (nonfluorescent) was prepared by hybridizing fluorescently labeled oligomer F and quencher-labeled oligomer Q mixed in 1:9 molar ratio. The arrays are incubated with solutions corresponding to oligomer F at concentrations between 50 and 0.5 nM. (A) Schematic of the process. (B) Plot of fluorescence intensity as a function of the concentration of FQ. (C) Fluorescence image of the paper device qualitatively showing the dependence of the fluorescence intensity on the concentration of FQ. The error bars represent one standard deviation ( $n = 7$ ).

are added to the ssDNA arrays on the surface of paper and allowed to incubate at 37 °C for 30 min. We are able to detect concentrations of DNA oligomer as low as 500 pM using paper-anchored arrays of ssDNA strands complementary to F.

### Characterization of Paper-Based DNA-Directed Antibody Arrays.

We formed DNA arrays by incubating solutions of ssDNA-conjugated rabbit IgG on disks (3 mm diameter) of paper on the surface of which ssDNA with complementary sequence had been synthesized. The dsDNA (formed from the hybridization of the two ssDNA strands) anchored the IgG to the surface of the paper.

Disks of untreated paper were used as controls. The surface of the disks was blocked with a BSA solution in PBS and then washed with PBS and hybridized with ssDNA-conjugated rabbit IgG (100 nM in PBS). Unbound conjugates were removed by washing three times with PBST buffer.

We used a fluorescently labeled antibody (DL549 anti-rabbit IgG) as a model analyte to test the performance of the array. DL549 anti-rabbit IgG in 10-fold dilutions (1 pM to 1 nM) in a solution of goat serum (10% serum in PBS) was added to each paper-anchored IgG array disk and incubated for 30 min.

The mean fluorescence intensity of both test and control zones was measured; Figure 4 shows the calibration data in the

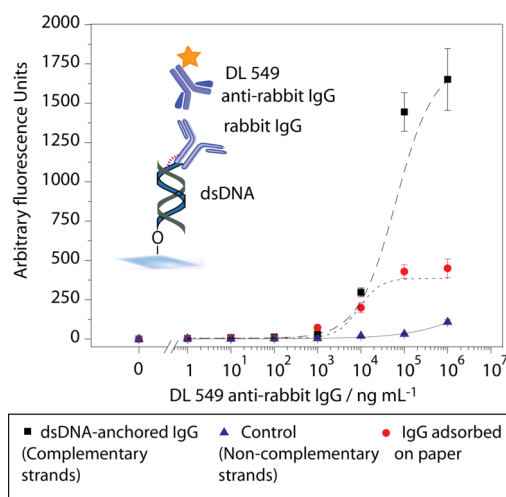


**Figure 4.** Detection of fluorescent goat anti-rabbit IgG in a solution of goat serum using a paper-anchored IgG array formed by the hybridization of ssDNA (sequence S2) synthesized directly on the surface of paper with complementary ssDNA-conjugated IgG (black squares). Paper-anchored ssDNA arrays with a sequence (S1) noncomplementary ssDNA-conjugated IgG served as a control (blue triangles). Red circles depict an immunoassay performed on untreated paper incubated with a solution of rabbit IgG and then blocked with a solution of BSA. Calibration plot of the output signal of the immunoassay versus the concentration of goat anti-rabbit IgG in the sample ( $N = 7$ ). The error bars represent one standard deviation. The dotted red arch indicates the use of a covalent linker to conjugate ssDNA to rabbit IgG.

form of the output fluorescent signal versus the concentration of DL549 anti-rabbit IgG in the sample. The LOD is  $\sim 10 \text{ ng mL}^{-1}$  (or  $\sim 67 \text{ pM}$ , defined as three times the standard deviation of the negative control) for the assay based on DNA arrays on paper.

Truncated sequences that occur following a failed coupling step, when capping renders them inactive in subsequent coupling cycles, occur as byproducts of the synthesis process. We designed the probes such that the target-binding region is located at the 5' end of the paper-anchored ssDNA. Because a majority of failed coupling steps occur in the early stages of the synthesis process (Figure 2), most truncations occur close to the 3' end and away from the target binding region and are not

expected to dramatically impact the specificity of the array. Although the coupling yield of our direct synthesis of oligonucleotide on paper was comparable with previously reported yields for in situ synthesized oligonucleotide arrays (95~99% per coupling step<sup>40,41</sup>), applications that require high specificity might require shorter synthesized probes.<sup>41</sup> This possible challenge could be circumvented in applications in which the detection of a single nucleotide polymorphism (SNP) is desired by targeting sequences peripheral to the SNP site.

#### ELISA Using Paper-Based DNA-Directed Antibody Arrays.

The ultimate goal behind developing the paper-anchored antibody array technique is to measure the levels of a clinically relevant protein in biological fluids from humans, animals, and plants. To do so, we assembled devices using paper-anchored arrays of capture antibody in microzones and used these devices to quantify levels of *hCRP* spiked into diluted human serum using a sandwich ELISA assay. We formed these antibody arrays by incubating solutions of ssDNA-conjugated anti-*hCRP* antibody on disks of paper on the surface of which ssDNA with complementary sequence had been synthesized. The dsDNA (formed from the hybridization of the two ssDNA strands) anchored the anti-*hCRP* antibody to the surface of the paper.

Diluted human serum samples were spiked with recombinant *hCRP* at concentrations ranging from 16 to 1000 pg mL<sup>-1</sup> and applied them to the microzones. We used a biotinylated anti-*hCRP* as detection antibody and streptavidin Cy5 as a fluorescent probe (see the [Experimental Section](#) in the [Supporting Information](#) for details). [Figure 5](#) shows the calibration curve

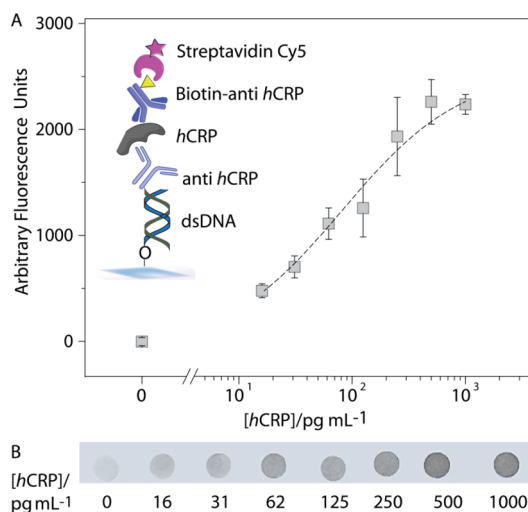


**Figure 5.** Device using paper-anchored ssDNA arrays for the detection of *hCRP* in a solution of human serum. (A) Calibration plot for fluorescence versus the concentration of *hCRP*. Each datum is the mean of seven replicates ( $N = 7$ ), and the error bars represent the standard deviations of the measurements. The signal of the blank (at zero concentration of spiked *hCRP*) was subtracted. Inset: schematic of the sandwich ELISA for *hCRP*. The capture antibody (anti-*hCRP*) is conjugated to a ssDNA strand complementary to the ssDNA strand synthesized on paper. The detection antibody is labeled with biotin (Biotin anti-*hCRP*). Streptavidin Cy5 is used to quantify the concentration of *hCRP*. (B) Images of the results using 16 to 100 pg mL<sup>-1</sup> concentrations of *hCRP*.

for the concentration of *hCRP* vs fluorescence intensity. The data were fit to Hill's equation with  $R^2 = 0.993$ . The LOD, defined as three times the standard deviation of the control at zero concentration of spiked analyte, was 17 pg mL<sup>-1</sup> ( $\sim 1$  pM).

#### Multiplexed Assay for the Detection of Fluorescently Labeled Nucleic Acids and Proteins.

To show that paper-anchored ssDNA arrays with different sequences can be used to assemble paper-based devices capable of detecting DNA and antibodies from a single sample, in the same device we used a solution containing a mixture of two model targets, a fluorescently labeled DNA oligomer, F, and a fluorescently labeled antibody, anti-rabbit IgG antibody conjugated to DL549. [Figure 6](#) shows a schematic of the process.

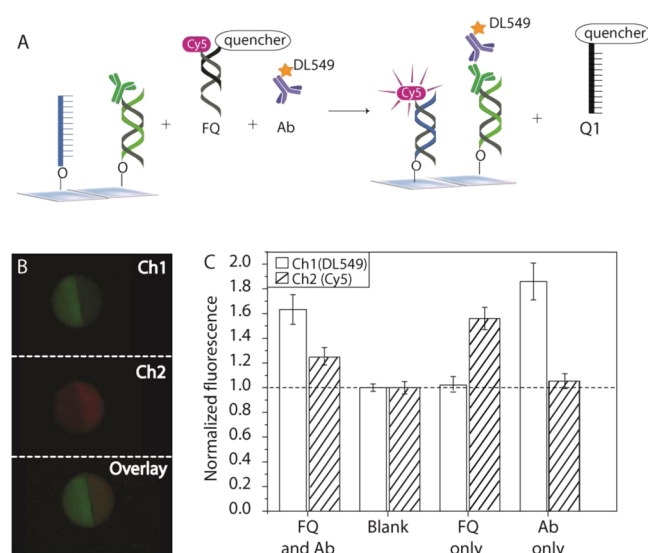


**Figure 6.** Device using paper-anchored ssDNA arrays for the multiplexed detection of fluorescently labeled nucleic acids and antibodies. (A) Schematic of the process. (B) Image of a device assembled using two paper-based arrays adjacent to each other and supported by vinyl plastic tape. The same device is scanned in both the Cy5 (Ch1, top) and Cy3 (Ch2, middle) fluorescence channels, and the signal is overlaid in the bottom image. (C) Fluorescence intensity obtained using seven independent devices when adding a mixture of FQ and Ab, buffer only, FQ only, or AB only to the device. In (C), the average fluorescence of the array probe is normalized to the average fluorescence intensity of the adjacent control array probe (i.e., the ratio of the signal from a probe to the signal related to nonspecific binding or cross-hybridization in the fluorescence channel and in the same device).

To prepare a paper-based analytical device that incorporates both ssDNA and protein arrays, we synthesized independently, on paper, ssDNA with orthogonal sequences S1 and S2 (see [Table S-1](#)) and shaped the paper strips into half-disks with 3 mm diameter by cutting. The array of ssDNA with sequence S1 was used without further modification to form the device. To form the protein array, we incubated the half disk of ssDNA with sequence S2 synthesized on its surface to a solution of complementary ssDNA-conjugated rabbit IgG; the dsDNA formed from the hybridization of the two ssDNA strands anchored the IgG to the surface of the paper. We placed the two half-disks on which ssDNA and protein arrays were formed adjacently to form a single continuous paper microzone and assembled a device as described in [Figure S-3](#). To prevent nonspecific adsorption, we blocked the surface of the paper using a solution of BSA (1% in PBS, pH 7.6) for 30 min.

The fluorescently labeled target oligomer F was prehybridized to the quencher-labeled oligomer Q, as described in the [Supporting Information](#). A solution containing a mixture of FQ

and anti-rabbit IgG antibody conjugated to DL549 (Ab), both at 5 nM concentration, was added to each device, incubated for 30 min at 37 °C, and allowed to cool to room temperature. The microzones were then washed three times with PBS and imaged with a fluorescence scanner.

Figure 6B shows an image of a typical device, and Figure 6C shows the average fluorescence data obtained using seven independent devices. The background fluorescence observed is likely caused by either the autofluorescence of the paper or by nonspecific adsorption of the bioanalytes on the surface of the paper. As tape is not present at the center of the device, we do not expect it to contribute to the background. We expect that lower concentrations of target molecules could be detected by using fluorescent detection probes with longer wavelengths (e.g., far red to near-IR) and a low degree of spectral overlap or by incorporating additional blocking and washing steps in the experimental design

## CONCLUSIONS

This work describes a method for assembling arrays of ssDNA and proteins on the surface of paper. The strategy is based on the synthesis of ssDNA directly on paper with modified 2'-deoxynucleoside phosphoramidites sequentially coupled to a growing oligonucleotide chain that is anchored in the hydroxyl groups present on the surface of cellulose paper.

This strategy of fabricating DNA arrays on paper is cost-effective because the crude product of the synthesis is sufficiently pure to allow us to specifically differentiate the complementary DNA strand from other sequences with minimal nonspecific interactions. This synthetic efficiency allows us to avoid distinct steps of DNA synthesis, purification, and immobilization; these steps are time-consuming and underlie the majority of the production costs (as a reflection of solvents and reagents).

Through hybridization with complementary strands of DNA, these DNA arrays can capture fluorescently labeled DNA, DNA-conjugated protein antigen, and DNA-conjugated antibodies. We demonstrate the use of these antibody arrays to perform a sensitive sandwich ELISA to detect human CRP (LOD 13 ng mL<sup>-1</sup>) and a multiplex assay capable of detecting DNA and antibodies in the same device. The versatility of this strategy offers new approaches to integration with simple microfluidic devices and of expansion of the repertoire of analyses, and the sensitivity of the assays, that can be conducted using paper.

## ASSOCIATED CONTENT

### Supporting Information

The Supporting Information is available free of charge on the ACS Publication Web site. The Supporting Information is available free of charge on the ACS Publications website at DOI: 10.1021/acs.analchem.5b02822.

Details of experimental methods, including materials and synthesized DNA sequences, direct synthesis of DNA on paper, characterization of synthesized DNA arrays, investigation of the yield of DNA synthesis on paper, design and fabrication of paper-based devices and formation of dsDNA arrays, procedures to form antibody-oligonucleotide conjugates and DNA-directed protein arrays, characterization of rabbit IgG arrays on paper, detection of hCRP on paper, immunoassays on untreated paper and standard polystyrene plates, multiplex detection of fluorescently labeled nucleic acids and antibodies on paper using ssDNA arrays, and PAGE gel of nondenatured and denatured IgG-DNA complexes (PDF)

## AUTHOR INFORMATION

### Corresponding Authors

\*E-mail: liu@chemistry.harvard.edu. Tel: 617 496-1067. Fax: 617 496-5688.

\*E-mail: gwhitesides@gmwgroup.harvard.edu. Tel: 617 495-9430. Fax: 617 495-9857.

### Author Contributions

†A.C.G. and J.N. contributed equally to this work.

### Notes

The authors declare no competing financial interest.

## ACKNOWLEDGMENTS

We are thankful for the financial support provided by the Bill and Melinda Gates Foundation under award 51308. A.C.G. was partially supported by DTRA Award No. HDTRA1-14-C-0037. J.N. was partially supported by an Eli Lilly Organic Chemistry Graduate Fellowship. F.G. acknowledges funding by the German Research Foundation (DFG) under contract GU 1468/1-1.

## REFERENCES

- (1) Walter, G.; Bussow, K.; Lueking, A.; Glokler, J. *Trends Mol. Med.* **2002**, *8*, 250–253.
- (2) Zhumabayeva, B.; Chenchik, A.; Siebert, P. D.; Herrler, M. *Adv. Biochem. Eng./Biotechnol.* **2004**, *86*, 191–213.
- (3) Miller, M. B.; Tang, Y. W. *Clin. Microbiol. Rev.* **2009**, *22*, 611–633.
- (4) Shin, Y. S.; Ahmad, H.; Shi, Q. H.; Kim, H.; Pascal, T. A.; Fan, R.; Goddard, W. A.; Heath, J. R. *ChemPhysChem* **2010**, *11*, 3063–3069.
- (5) Barbulovic-Nad, I.; Lucente, M.; Sun, Y.; Zhang, M.; Wheeler, A. R.; Bussmann, M. *Crit. Rev. Biotechnol.* **2006**, *26*, 237–259.
- (6) Dufva, M. *Biomol. Eng.* **2005**, *22*, 173–184.
- (7) Taylor, S.; Smith, S.; Windle, B.; Guiseppi-Elie, A. *Nucleic Acids Res.* **2003**, *31*, e87–e87.
- (8) Martinez, A. W.; Phillips, S. T.; Butte, M. J.; Whitesides, G. M. *Angew. Chem., Int. Ed.* **2007**, *46*, 1318–1320.
- (9) Martinez, A. W.; Phillips, S. T.; Carrilho, E.; Thomas, S. W.; Sindi, H.; Whitesides, G. M. *Anal. Chem.* **2008**, *80*, 3699–3707.
- (10) Martinez, A. W.; Phillips, S. T.; Nie, Z.; Cheng, C. M.; Carrilho, E.; Wiley, B. J.; Whitesides, G. M. *Lab Chip* **2010**, *10*, 2499–2504.
- (11) Martinez, A. W.; Phillips, S. T.; Whitesides, G. M. *Proc. Natl. Acad. Sci. U. S. A.* **2008**, *105*, 19606–19611.
- (12) Martinez, A. W.; Phillips, S. T.; Whitesides, G. M.; Carrilho, E. *Anal. Chem.* **2010**, *82*, 3–10.
- (13) Liu, H.; Crooks, R. M. *J. Am. Chem. Soc.* **2011**, *133*, 17564–17566.
- (14) Liu, H.; Li, X.; Crooks, R. M. *Anal. Chem.* **2013**, *85*, 4263–4267.
- (15) Vella, S. J.; Beattie, P.; Cademartiri, R.; Laromaine, A.; Martinez, A. W.; Phillips, S. T.; Mirica, K. A.; Whitesides, G. M. *Anal. Chem.* **2012**, *84*, 2883–2891.
- (16) Wang, S.; Ge, L.; Song, X.; Yu, J.; Ge, S.; Huang, J.; Zeng, F. *Biosens. Bioelectron.* **2012**, *31*, 212–218.
- (17) Yetisen, A. K.; Akram, M. S.; Lowe, C. R. *Lab Chip* **2013**, *13*, 2210–2251.
- (18) Credou, J.; Berthelot, T. *J. Mater. Chem. B* **2014**, *2*, 4767–4788.
- (19) Kong, F.; Hu, Y. F. *Anal. Bioanal. Chem.* **2012**, *403*, 7–13.
- (20) Bailey, R. C.; Kwong, G. A.; Radu, C. G.; Witte, O. N.; Heath, J. R. *J. Am. Chem. Soc.* **2007**, *129*, 1959–1967.
- (21) Boozer, C.; Ladd, J.; Chen, S.; Jiang, S. *Anal. Chem.* **2006**, *78*, 1515–1519.
- (22) Fan, R.; Vermesh, O.; Srivastava, A.; Yen, B. K. H.; Qin, L. D.; Ahmad, H.; Kwong, G. A.; Liu, C. C.; Gould, J.; Hood, L.; Heath, J. R. *Nat. Biotechnol.* **2008**, *26*, 1373–1378.
- (23) Boozer, C.; Ladd, J.; Chen, S.; Yu, Q.; Homola, J.; Jiang, S. *Anal. Chem.* **2004**, *76*, 6967–6972.
- (24) Angenendt, P.; Glokler, J.; Sobek, J.; Lehrach, H.; Cahill, D. J. *Journal of Chromatography A* **2003**, *1009*, 97–104.

- (25) Bailey, R. C.; Kwong, G. A.; Radu, C. G.; Witte, O. N.; Heath, J. *R. J. Am. Chem. Soc.* **2007**, *129*, 1959–1967.
- (26) Benters, R.; Niemeyer, C. M.; Drutschmann, D.; Blohm, D.; Wohrle, D. *Nucleic Acids Res.* **2002**, *30* (e10), 1–7.
- (27) Boozer, C.; Ladd, J.; Chen, S. F.; Jiang, S. T. *Anal. Chem.* **2006**, *78*, 1515–1519.
- (28) Douglas, E. S.; Chandra, R. A.; Bertozzi, C. R.; Mathies, R. A.; Francis, M. B. *Lab Chip* **2007**, *7*, 1442–1448.
- (29) Dufva, M. *Biomol. Eng.* **2005**, *22*, 173–184.
- (30) Fan, R.; Vermesh, O.; Srivastava, A.; Yen, B. K. H.; Qin, L.; Ahmad, H.; Kwong, G. A.; Liu, C.-C.; Gould, J.; Hood, L.; Heath, J. R. *Nat. Biotechnol.* **2008**, *26*, 1373–1378.
- (31) Schroeder, H.; Adler, M.; Gerigk, K.; Muller-Chorus, B.; Gotz, F.; Niemeyer, C. M. *Anal. Chem.* **2009**, *81*, 1275–1279.
- (32) Wacker, R.; Schroder, H.; Niemeyer, C. M. *Anal. Biochem.* **2004**, *330*, 281–287.
- (33) Beaucage, S. L.; Iyer, R. P. *Tetrahedron* **1992**, *48*, 2223–2311.
- (34) Agrawal, S. *Protocols for Oligonucleotides and Analogs: Synthesis and Properties*; Springer, 1993; Vol. 20.
- (35) Glavan, A. C.; Martinez, R. V.; Subramaniam, A. B.; Yoon, H. J.; Nunes, R. M. D.; Lange, H.; Thuo, M. M.; Whitesides, G. M. *Adv. Funct. Mater.* **2014**, *24*, 60–70.
- (36) Proudnikov, D.; Timofeev, E.; Mirzabekov, A. *Anal. Biochem.* **1998**, *259*, 34–41.
- (37) Glavan, A. C.; Martinez, R. V.; Subramaniam, A. B.; Yoon, H. J.; Nunes, R. M. D.; Lange, H.; Thuo, M. M.; Whitesides, G. M. *Adv. Funct. Mater.* **2014**, *24*, 60.
- (38) Donoso, M. G.; Méndez-Vilas, A.; Bruque, J. M.; González-Martin, M. L. *Int. Biodeterior. Biodegrad.* **2007**, *59*, 245–251.
- (39) ATDBIO. “Solid-Phase Oligonucleotide synthesis”, retrieved at <http://www.atdbio.com/content/17/Solid-phase-oligonucleotide-synthesis>, 2014.
- (40) Agbavwe, C.; Kim, C.; Hong, D.; Heinrich, K.; Wang, T.; Somoza, M. J. *Nanobiotechnol.* **2011**, *9*, 57.
- (41) Nuwaysir, E. F.; Huang, W.; Albert, T. J.; Singh, J.; Nuwaysir, K.; Pitas, A.; Richmond, T.; Gorski, T.; Berg, J. P.; Ballin, J.; McCormick, M.; Norton, J.; Pollock, T.; Sumwalt, T.; Butcher, L.; Porter, D.; Molla, M.; Hall, C.; Blattner, F.; Sussman, M. R.; Wallace, R. L.; Cerrina, F.; Green, R. D. *Genome Res.* **2002**, *12*, 1749–1755.